Supporting Information

Dissecting the intracellular signalling and fate of a DNA nanosensor by super-resolution and quantitative microscopy

Agata Glab,[†] Alessandro Bertucci,[‡] Fabiana Martino,[#] Marcin Wojnilowicz,[†] Alessia Amodio,[†,‡] Mariano Venanzi,[‡] Francesco Ricci,[‡] Giancarlo Forte,[#] Frank Caruso,*[,†] and Francesca Cavalieri*[,†,‡]

[†]ARC Centre of Excellence in Convergent Bio-Nano Science and Technology, and the Department of Chemical Engineering, The University of Melbourne, Parkville, Victoria 3010, Australia

[‡]Dipartimento di Scienze e Tecnologie Chimiche, Università degli Studi di Roma Tor Vergata, Via della Ricerca Scientifica 1, 00133, Rome, Italy

[#]International Clinical Research Center (ICRC), St Anne's University Hospital, CZ-65691 Brno, Czech Republic

Corresponding Authors

*E-mail: francesca.cavalieri@unimelb.edu.au; fcaruso@unimelb.edu.au

Table of Contents

Section S5. Enzyme-linked immunosorbent assay (ELISA).

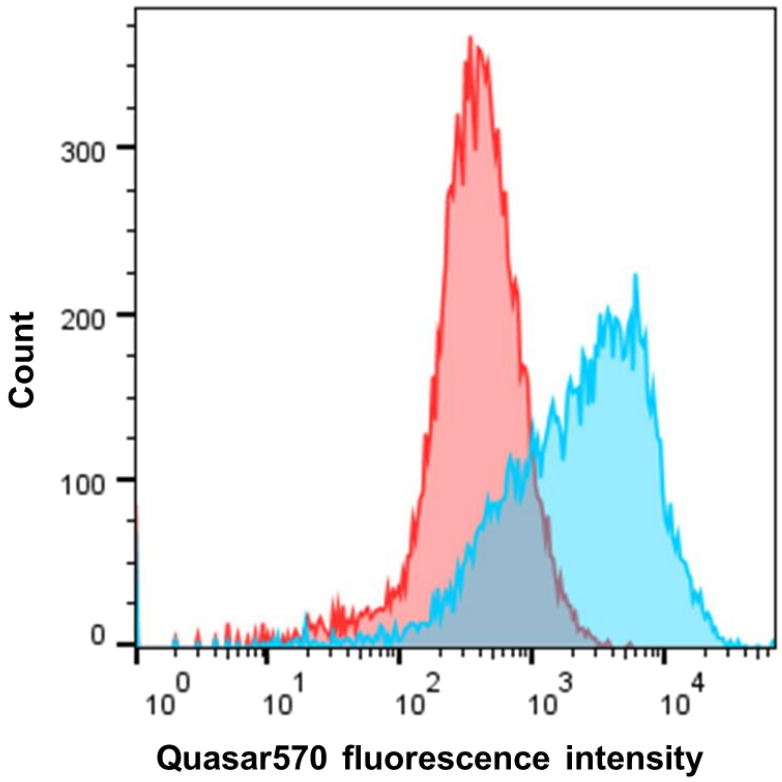

Figure S1. Flow cytometry profiles of PC3 cells transfected with 50 nM Nanowsitch$_{\text{NF-κB}}$ (blue) and non-treated cells (red). The fluorescence intensity measured refers to Quasar570 emission.

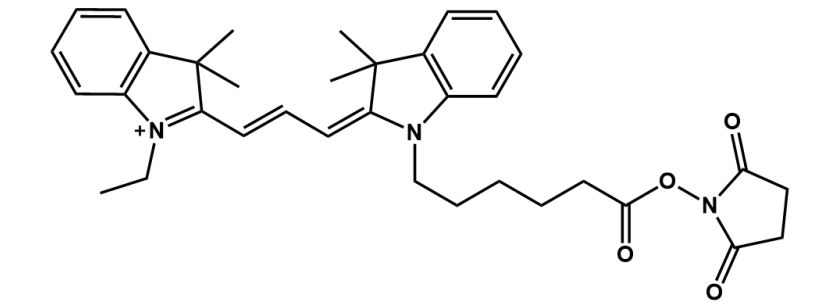

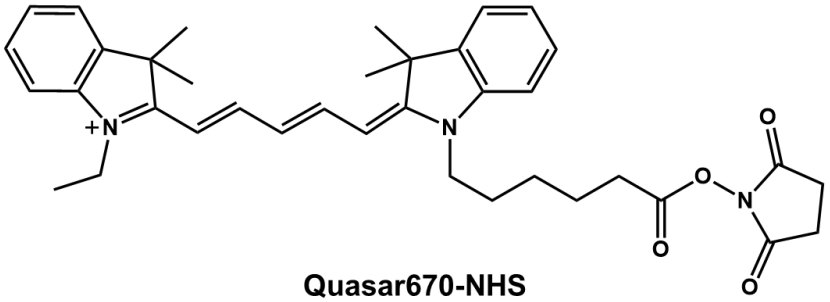

Figure S2. Chemical structures of Quasar570 and Quasar670 succinimidyl esters, which were used as oligonucleotide chromophores for FRET.

Section S1. Design of Nanoswitch$_{\text{NF-κB}}$ and control FRET sequence.

The structure of the Nanoswitch$_{\text{NF-κB}}$ features the double-strand binding domain composed of the sequence 5′-GGGACTTTCC-3′ and its complementary counterpart. Using mfold software (http://unafold.rna.albany.edu/?q=mfold), it is possible to analyse the DNA populated conformations and their thermodynamic properties. The single-stranded DNA sequence of the Nanoswitch$_{\text{NF-κB}}$ presents two distinct conformers in thermodynamic equilibrium, as depicted in Figure 1. Based on the mfold simulation, the free energy of the two states in equilibrium can be evaluated. At 37 °C, the unbound FRET HIGH state has a Gibbs free energy, ΔG^0 of −10.55 kcal/mol, whereas the binding-competent FRET LOW state has a ΔG^0 of −10.47 kcal/mol.

As a control FRET sequence, a DNA nanostructure was designed featuring the same conformations as those of the Nanoswitch$_{\text{NF-κB}}$ but lacking the binding motif. Thus, this particular design is unable to undergo switching equilibrium. The double stem–loop conformation of this control sequence has a ΔG^0 of −10.84 kcal/mol at 37° C, which is comparable with the free energy of the FRET HIGH state of the Nanoswitch$_{\text{NF-κB}}$. To rule out possible competitive interactions of the Nanoswitch$_{\text{NF-κB}}$ with mRNA sequences present in the cytosol, the Basic Local Alignment Search Tool (BLAST, National Center for Biotechnology Information) was used. Investigation using the BLAST analysis tool was performed against the complementary sequence of the Nanoswitch$_{\text{NF-κB}}$ and control FRET sequence (see Figure S3, Figure S4). The estimated ΔG^0 values of the Nanoswitch$_{\text{NF-κB}}$, control FRET sequence in the double stem–loop and hairpin conformations and the double strands hybridised with the most similar sequence obtained with the BLAST analysis (e.g. the first sequence after the query sequence in Figures S3, S4, respectively) are reported in Table S1.

The comparison between the ΔG^0 values confirmed that possible competitive interactions involving the Nanoswitch$_{\text{NF-κB}}$ and endogenous mRNAs, can be neglected (see Figure S3, Figure S4 and Table S1). We further confirmed that the Nanoswitch$_{\text{NF-κB}}$ does not provide an interfering fluorescence signal in the presence of complementary nucleic acids molecules when present at concentrations similar to the intracellular concentration of mRNA (pM).[31] Fluorescence emission spectra were obtained upon incubation of 50 nM Nanoswitch$_{\text{NF-κB}}$ with 0.09 nM Nanoswitch$_{\text{NF-κB}}$ complementary strand (5′- TCAAATAAGTATGGAAAGTCC-3′). The signal was monitored for

60 min after the addition of the complementary strand. No significant increase in signal was noticed, indicating lack of interfering signal.

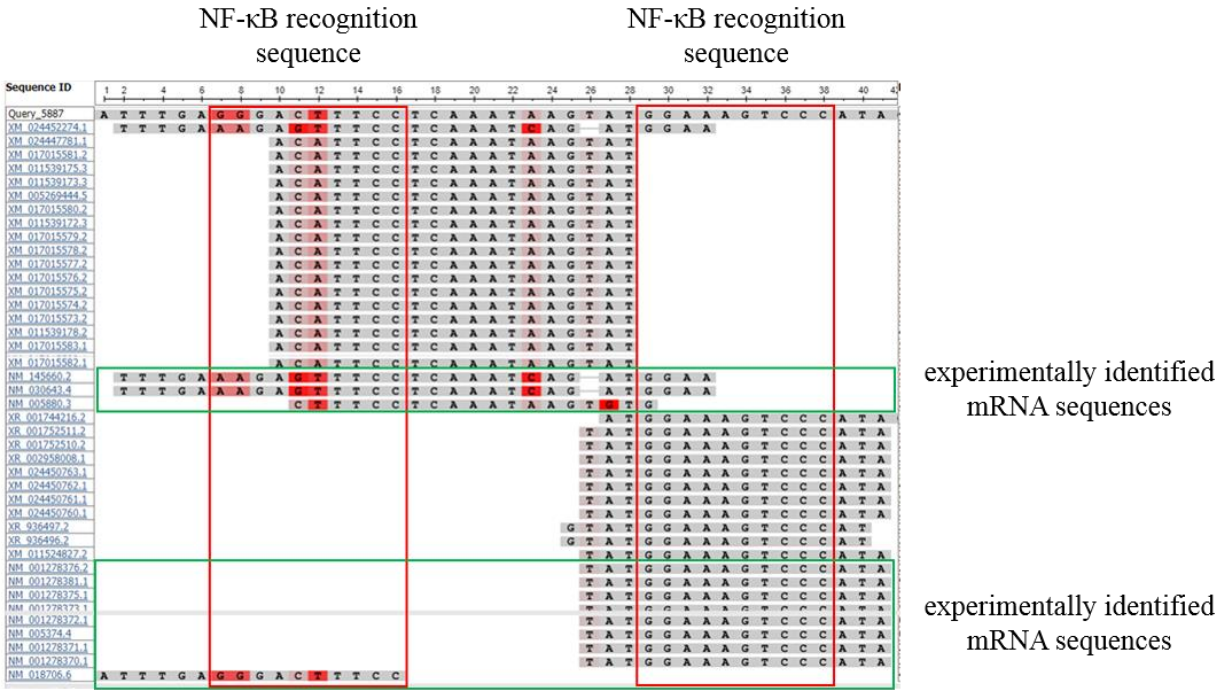

Figure S3. Multiple Sequence Aligner (MSA) visualisation BLAST analysis of Nanoswitch$_{\text{NF-κB}}$ complementary sequence. In the first column, the sequence ID (accession number) is reported and in the second column, the sequence is reported. The parameter selection for the analysis was: database "Reference RNA sequences", organism "human" and optimised for "somewhat similar sequences (blastn)". The first row contains the query sequence (query_5887). In the second row, the first blast hit is reported. The bases enclosed in the red boxes represent the ones of the recognition sequence for NF-κB proteins in the binding form. The results enclosed in the green boxes represent the non-predicted mRNA sequences identified by the analysis (12 out of 41), corresponding to the experimentally identified mRNA sequences, whereas predicted sequences are sequences predicted by automated computational analysis. Bases highlighted in dark red represent mismatch, whereas the ones highlighted in light red represent a perfect match after a mismatch in the previous blast hit sequence.

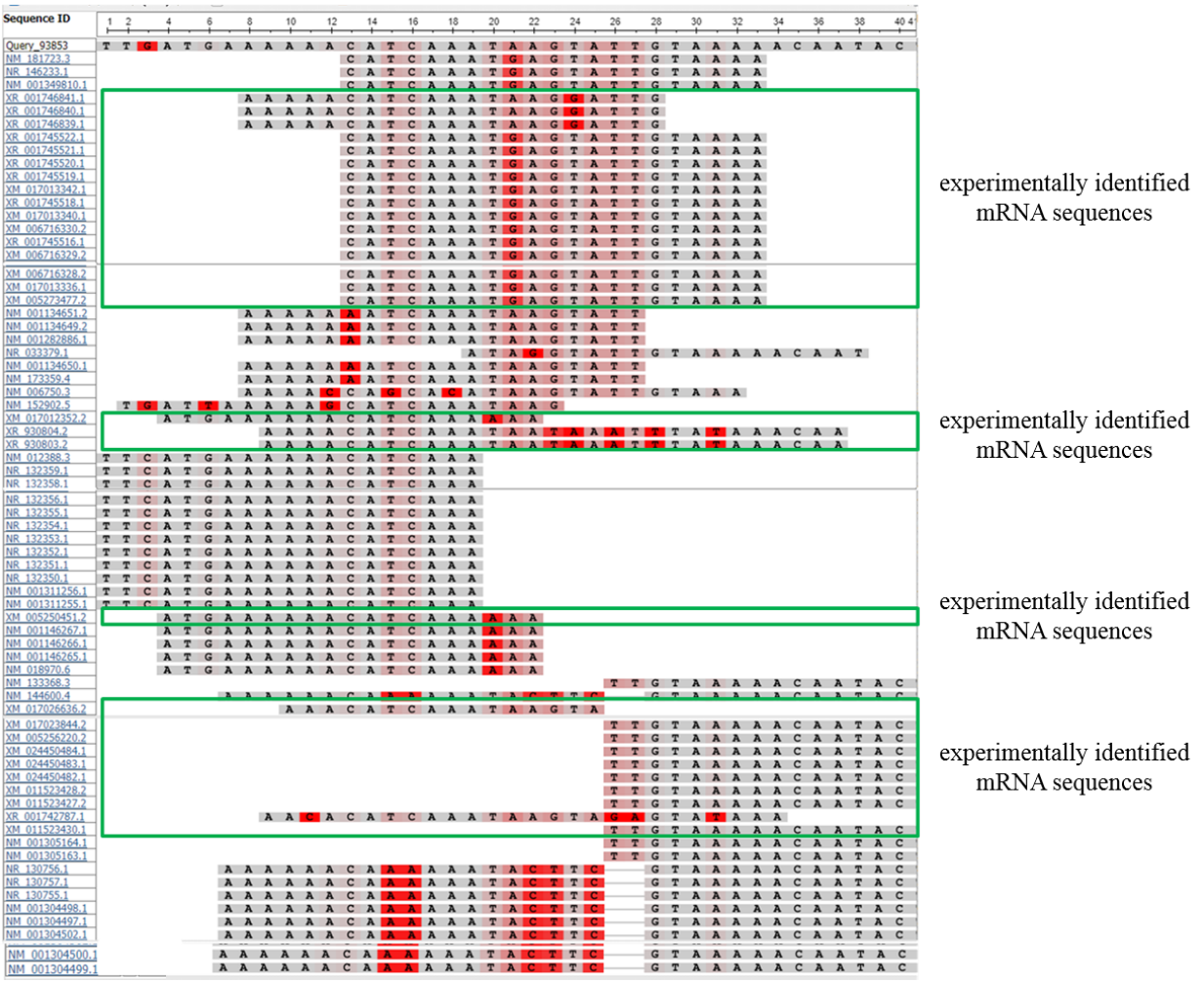

Figure S4. MSA visualisation BLAST analysis of control FRET complementary sequence. In the first column, the sequence ID is reported (accession number) and in the second column, the sequence of the query nucleotide is reported. The parameter selection for the analysis was: database "Reference RNA sequences", organism "human" and optimised for "somewhat similar sequences (blastn)". The first row contains the query sequence (query_93853). The results enclosed in the green boxes represent the non-predicted mRNA sequences (i.e. experimentally identified mRNA sequences) identified by the analysis (30 out of 69). Bases highlighted in dark red represent mismatch, whereas the ones highlighted in light red represent a perfect match after a mismatch in the previous blast hit sequence.

Table S1. Comparison between the estimated ΔG^0 values of the Nanoswitch$_{\mathbf{NF\text{-}\kappa B}}$ and control FRET sequence in the double stem–loop and hairpin conformations and the double strands hybridised with the most similar sequence obtained with the BLAST analysis (e.g. the first sequence after the query sequence in Figures S3, S4, respectively)[a].

Species	**ΔG^0 [kcal/mol]**
Nanoswitch$_{\mathbf{NF\text{-}\kappa B}}$ non-binding state	-10.55
Nanoswitch$_{\mathbf{NF\text{-}\kappa B}}$ binding-competent state	-10.47
Nanoswitch$_{\mathbf{NF\text{-}\kappa B}}$/first BLAST hit	-0.55
Control FRET sequence	-10.84
Control FRET sequence/first BLAST hit	-0.54

[a]Using NUPACK,[1] the ΔG^0 values of the different species at equilibrium at 37 °C were determined using 1 μM as the starting concentration for all reagents.

Section S2. FRET efficiency measurements.

The FRET efficiency ($FRET_{solution}$) in solution was calculated using Equation (S1):

$$FRET_{solution}\,[\%] = \frac{I_{max} - I_{DA}}{I_{max}} \times\ 100\ \% \tag{S1}$$

where I_{DA} is the donor fluorescence intensity measured during the titration experiments (Figure 2 and S5). I_{max} is the maximum donor fluorescence emission. I_{max} was measured by treating the Nanoswitch$_{\textbf{NF-κB}}$ with DNase I, which resulted in degradation of the probe and complete loss of energy transfer between the fluorophore pair (Figure S7).

The data were also plotted in terms of normalised signal gain (NSG) against NF-κB concentration. NSG was calculated using Equation (S2), where R is the donor-to-acceptor fluorescence intensity ratio at a given protein concentration:

$$NSG = \frac{R - R_{min}}{R_{max} - R_{min}} \tag{S2}$$

To obtain K_D for the binding process, the data were fitted with a Langmuir-type binding model in GraphPad Prism software using Equation (S3):

$$NSG = \frac{D_{tot} + P_{tot} + K_D - \sqrt{(D_{tot} + P_{tot} + K_D)^2 - 4D_{tot}P_{tot}}}{2D_{tot}} \tag{S3}$$

where D_{tot} is the total concentration of the Nanoswitch$_{\textbf{NF-κB}}$ and P_{tot} is the total concentration of NF-κB protein.

K_S values were estimated assuming that the Nanoswitch$_{\textbf{NF-κB}}$ exists in two discrete conformations, each associated with a distinct FRET value determined experimentally. In the double stem–loop conformation, the donor is quenched by both contact and FRET effects (i.e., $FRET_{non\text{-}binding}$ = 90%) (Figure S8). In contrast, in the hairpin conformation, the donor featured a FRET value similar to that measured in the fully bound states (i.e., $FRET_{binding\ or\ bound}$ = 20%) (Figure 2B and S5B). Hence, the intrinsic FRET values observed for the Nanoswitch$_{\textbf{NF-κB}}$ arise from the linear combination of these two extreme energy transfer conditions. The fractional concentration of the two conformational states (x and $1 - x$) can be calculated using Equation (S4):

$$FRET_{exp}(\%) = \big(0.9x + 0.2(1 - x)\big) \times 100\% \tag{S4}$$

Thus, K_S values of 1.0 and 1.2 were estimated at 37 °C for measurements in PBS and PEG/PBS, respectively.

Assuming that only a particular Nanoswitch$_{\mathbf{NF\text{-}\kappa B}}$ conformer binds to either p50/p50 or p50/p65, the observed dissociation constant, K_D^{obs}, can be determined assuming a Langmuir-type one-site binding process, combined with an intrinsic conformational K_S as follows, where K_D^{int} is the intrinsic dissociation constant:

$$K_D^{obs} = K_D^{int} \frac{1+K_S}{K_S} \quad \text{(S5)}$$

Assuming that in the FRET LOW state, only the Förster mechanism is operative, the Donor-Acceptor (D-A) distance R_{DA} could be estimated through the Equation (S6):

$$R = R_0 \left(\frac{1}{E} - 1\right)^{\frac{1}{6}} \quad \text{(S6)}$$

where R_0 is the Förster distance, a parameter purely dependent on the spectroscopic properties of the D-A pair. In the case of the Quasar 570/Quasar 670 pair, we obtained R_0=53.4 Å. For the determination of R_0, the donor (Quasar 570) quantum yield (ϕ_D=0.22) was obtained with respect to the reference quantum yield of Rhodamine 6G, the overlap integral ($J=5.62 \cdot 10^{15}$ M^{-1} cm^{-1} nm^4) was calculated from the emission spectrum of Quasar 570 and absorption spectrum of Quasar 670, and a κ^2 value of 2/3 (dynamic average orientation between the D/A pair) was assumed.

FRET measurements in cells imaging were performed using Nikon A1R confocal microscope. First, the regions of interest, which contained either whole cell, nucleus, or cytoplasm, were designed (Figure S11). Then, the fluorescence intensity of the Nanoswitch$_{\mathbf{NF\text{-}\kappa B}}$ or control FRET sequence (I_D) was measured by exciting the donor (Quasar 570) at λ_{ex} = 561 nm. Subsequently, the acceptor (Quasar 670) was excited at λ_{ex} = 640 nm and bleached using maximum laser power. Finally, the donor was excited at λ_{ex} = 561 nm and the change in the fluorescence intensity was measured (I_{Db}). Based on the obtained data, the FRET efficiency ($FRET_{cells}$) in cells was calculated using Equation (S7):

$$FRET_{cells} = \frac{I_{Db}-I_D}{I_{Db}} \times 100\ \% \quad \text{(S7)}$$

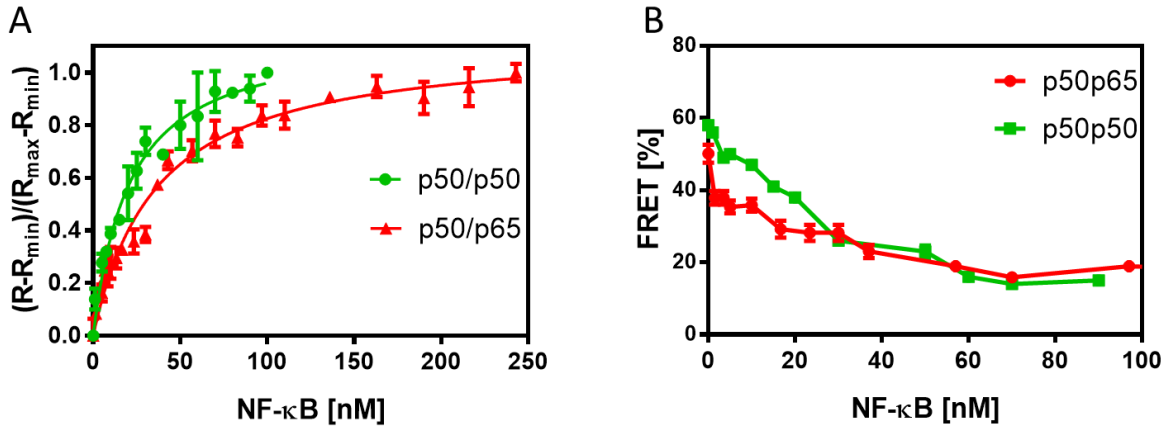

Figure S5. (A) Binding curves of the Nanoswitch$_{\text{NF-κB}}$ (5 nM) for the target proteins in PBS. (B) Variation in the FRET efficiency of the Nanoswitch$_{\text{NF-κB}}$ (5 nM) as a function of p50/p65 concentration (red) and p50/p50 concentration (green). All the measurements were performed at 37 °C. Error bars represent standard deviations, n = 3.

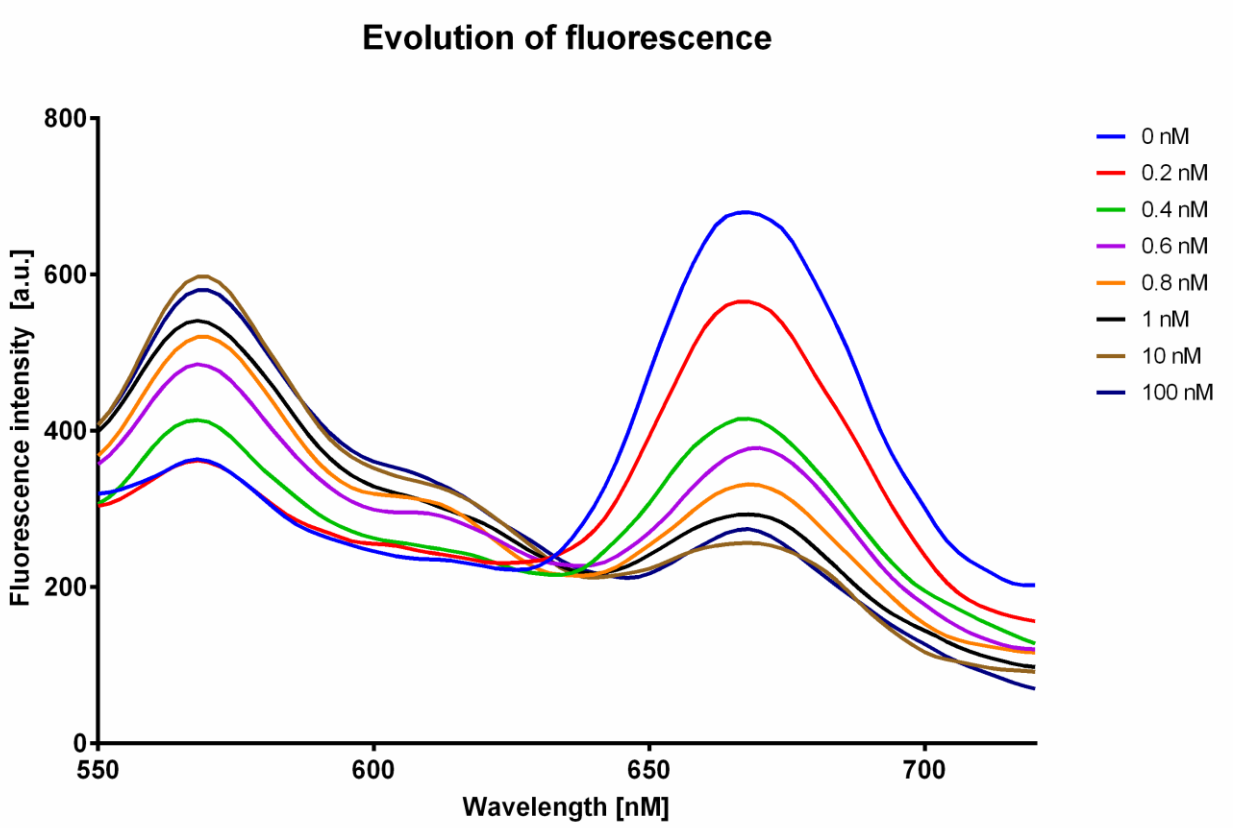

Figure S6. Fluorescence emission spectra of Nanoswitch$_{\text{NF-κB}}$ (5 nM) in the presence of increasing concentrations of NF-κB p50/p65 from 0 to 100 nM. As the concentration of NF-κB increases, the Nanoswitch$_{\text{NF-κB}}$ equilibrium shifts towards the binding-competent state, in which the two fluorophores, Quasar570 and Quasar670, are set apart. Therefore, the FRET signal decreases, which corresponds to an increase in donor (Quasar570) fluorescence and a decrease in the acceptor (Quasar670) fluorescence. λex = 520 nm, (PEG)/PBS (30% w/w), 37 °C.

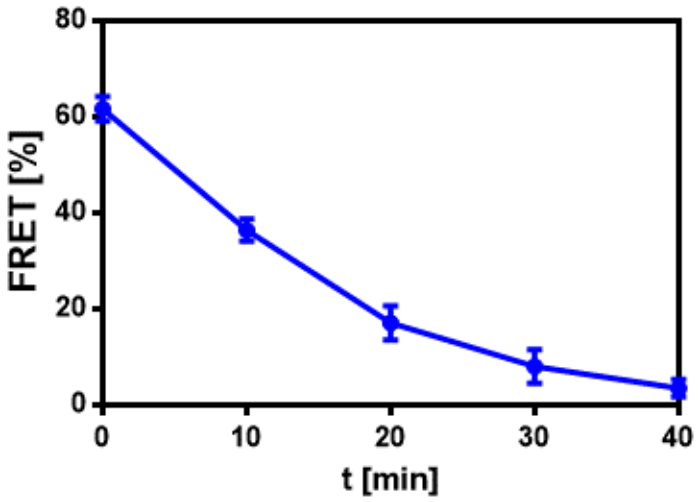

Figure S7. Variation in the FRET efficiency of the Nanoswitch$_{\text{NF-κB}}$ (5 nM) after treatment with DNAse I in PBS measured as a function of time. Before DNAse treatment, the FRET efficiency in Nanoswitch$_{\text{NF-κB}}$ was around 60%. Upon Nanoswitch$_{\text{NF-κB}}$ degradation, the fluorophores are not in contact anymore, resulting with the FRET and contact quenching disappearing. As a result, the FRET efficiency significantly decreases. λ_{ex} = 520 nm, PBS buffer, 37 °C. Error bars represent standard deviations, n = 3.

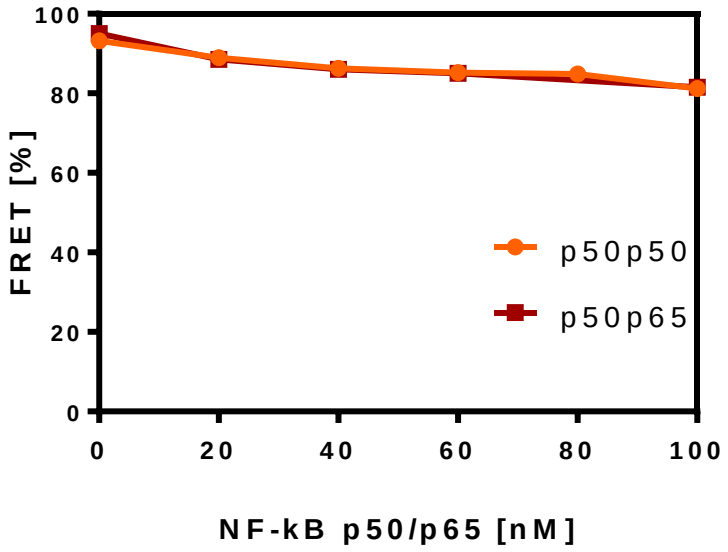

Figure S8. Changes in FRET efficiency for the control FRET sequence (5 nM) as a function of p50/p50 concentration (orange) and p50/p65 concentration (brown) measured at 37 °C in PBS. Error bars represent standard deviations, $n = 3$.

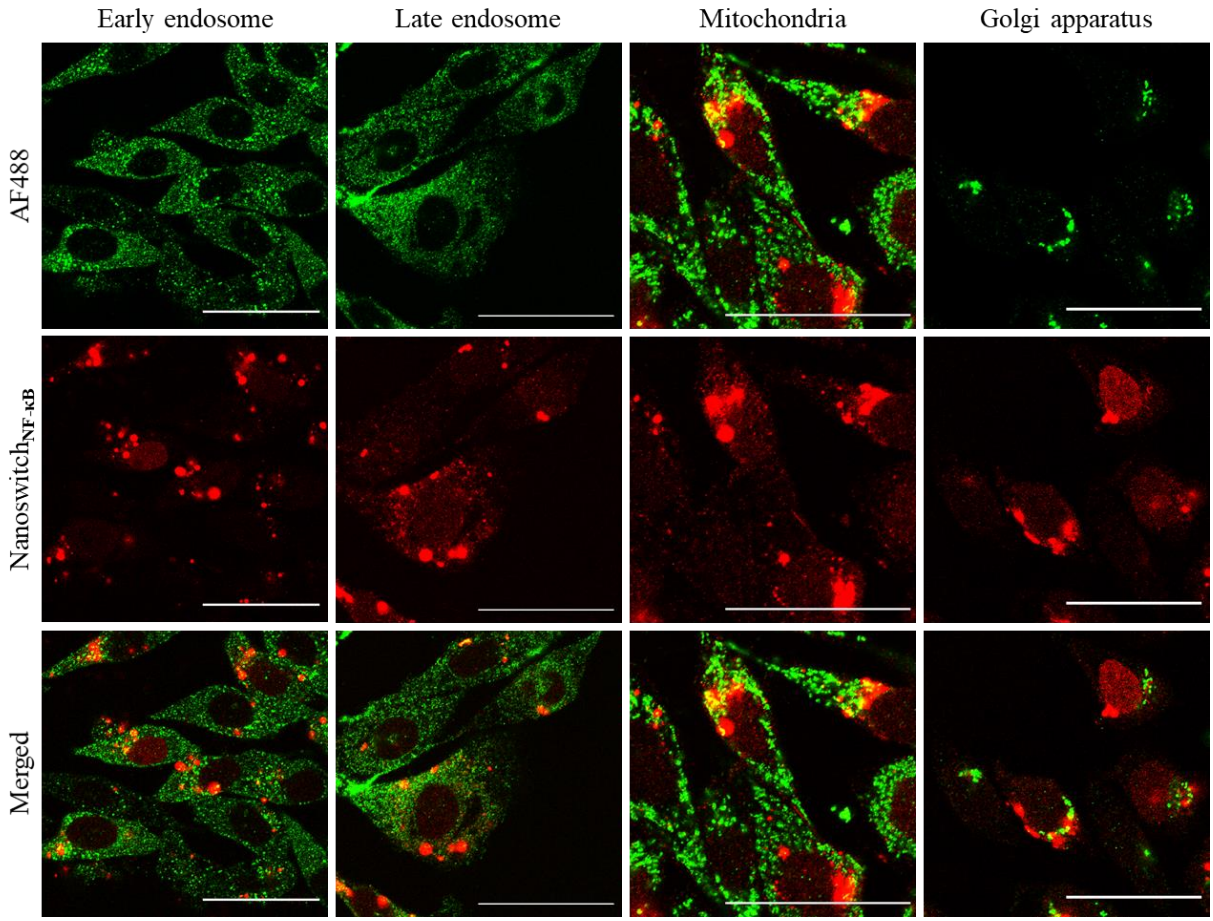

Figure S9. Colocalisation studies of Nanoswitch$_{NF-κB}$ with early and late endosomes, mitochondria and Golgi apparatus in PC3 cells using confocal microscopy. Photos were taken 24 h after transfection with 50 nM Nanoswitch$_{NF-κB}$ (red). Staining was performed using rabbit anti-EEA1 monoclonal antibody (early endosome), rabbit anti-Rab7 monoclonal antibody (late endosome), rabbit anti-Tom20 monoclonal antibody (mitochondria) or rabbit anti-GM130 monoclonal antibody (Golgi apparatus) followed by a secondary goat anti-rabbit AF488 conjugated antibody. Scale bars = 50 μm.

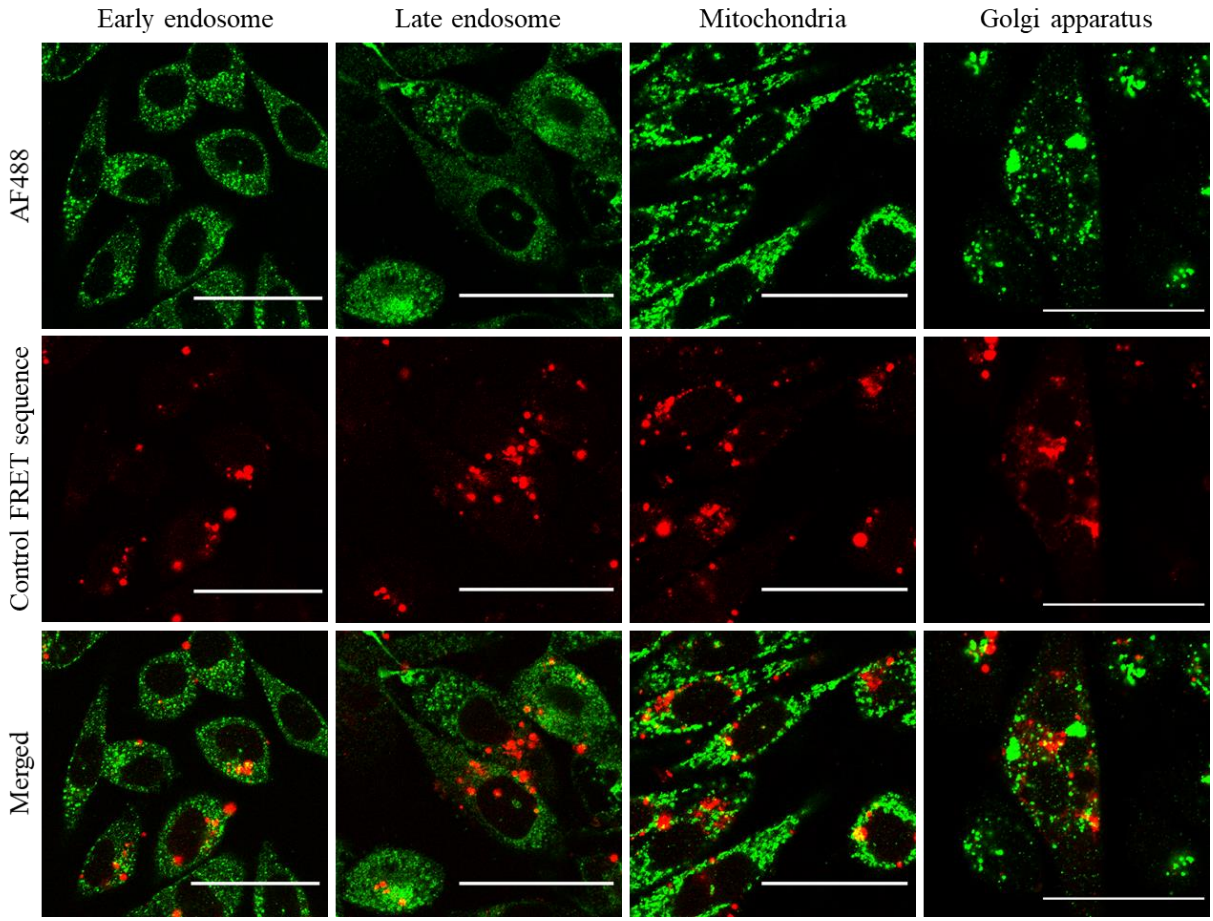

Figure S10. Colocalisation studies of control FRET sequence with early and late endosomes, mitochondria and Golgi apparatus in PC3 cells using confocal microscopy. Photos were taken 24 h after transfection with 50 nM control FRET sequence (red). Staining was performed using rabbit anti-EEA1 monoclonal antibody (early endosome), rabbit anti-Rab7 monoclonal antibody (late endosome), rabbit anti-Tom20 monoclonal antibody (mitochondria) or rabbit anti-GM130 monoclonal antibody (Golgi apparatus) followed by a secondary goat anti-rabbit AF488 conjugated antibody. Scale bars = 50 μm.

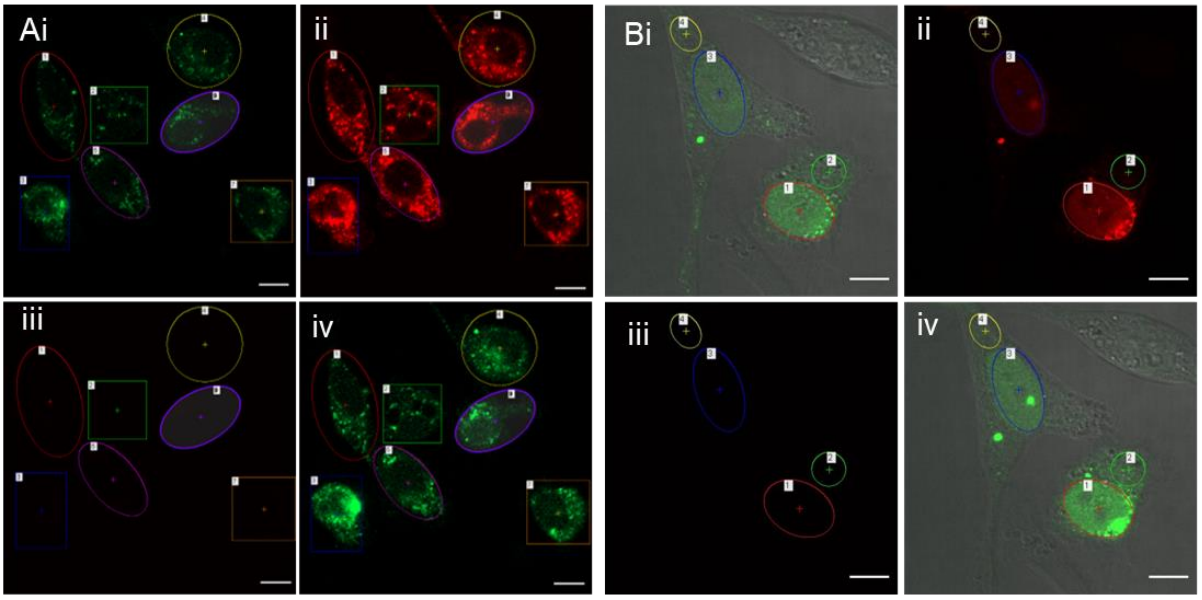

Figure S11. FRET experimental layout in cells (A) without and (B) with signals in the nucleus: (i) a number of regions of interest were selected, the donor (Quasar 570, green) was excited and its emission intensity was quantified; (ii) the acceptor (Quasar 670, red) was imaged and (iii) photobleached; (iv) the donor (Quasar 570, green) was excited and its emission intensity was quantified. The FRET efficiency was calculated by the relative variation in donor emission before and after photobleaching. Scale bars = 10 μm.

Section S3. siRNA mediated knocking down NF-κB expression followed by Nanoswitch$_{NF-κB}$ transfection.

siRNA-mediated NF-κB downregulation

Human prostate cancer PC3 cells were plated on Nunc™ Lab-Tek™ II chambered coverglass (Life Technologies, Scoresby, Australia) at a seeding density of 4 × 104 cells per well in 500 µL of DMEM medium supplemented with 10% FBS and incubated at 37 °C in 5% CO_2 overnight. Then, transfection with siRNA-targeting NF-κB was performed in OPTI-MEM reduced serum medium using lipofectamine RNAiMAX as a carrier according to supplier protocol with final RNA concentrations of 25 and 50 nM. After incubation for 12 h with siRNA/Lipofectamine RNAiMAX complexes, the transfection medium was discarded and replaced with 1 mL of fresh 10%FBS/DMEM, followed by incubation for 36 h. Then, the cells were counter-transfected with NanoswitchNF-κB with a final DNA concentration of 25 nM, and intracellular FRET measurements were performed according to the above described protocol.

Western Blot analysis of siRNA-mediated NF-κB downregulation in PC3 cells

Human prostate cancer PC3 cells were plated on a 12-well plate (Costar 3513, Corning, MA, USA) at a seeding density of 10^5 cells per well in 1 mL of DMEM medium supplemented with 10% FBS and incubated at 37 °C in 5% CO_2 overnight. Then, transfection with siRNA-targeting NF-κB was performed in OPTI-MEM reduced serum medium using lipofectamine RNAiMAX as a carrier according to supplier protocol with final RNA concentrations of 25 and 50 nM. After incubation for 12 h with siRNA/lipofectamine RNAiMAX complexes, the transfection medium was discarded and replaced with 1 mL of fresh 10%FBS/DMEM, followed by incubation for 36 h. Then, the cells were washed twice with D-PBS, trypsinised, washed again twice with D-PBS, and centrifuged (400 *g*, 5 min). Whole cell extract was prepared by adding RIPA buffer containing protease inhibitor cocktail to cells, followed by incubation for 30 min on ice. Then, cells were centrifuged (16000 *g*, 10 min, 4 °C) and the supernatant containing protein was transferred to a fresh tube. The protein extract (50 µg) was separated by sodium dodecyl sulphate–polyacrylamide gel electrophoresis and transferred onto a polyvinylidene membrane using standard protocols. The membrane was washed twice with PBS and incubated for 1 h with blocking buffer (5% w/v skim milk in 0.1% Tween20/PBS). Then, the membrane was washed four times with 0.1% Tween20-PBS, followed by overnight incubation with rabbit anti-NF-kB (1:2500)

and anti-β-actin (1:5000) primary antibodies in 5%BSA/0.1% Tween20/PBS. Next, the membrane was incubated with anti-rabbit peroxidase-conjugated antibody (1:5000 in 0.1% Tween20/PBS). The presence of antibodies was detected using Clarity Max Western ECL substrate and the antibodies were imaged with a ChemiDoc XRS+ imaging system (BioRad, USA).

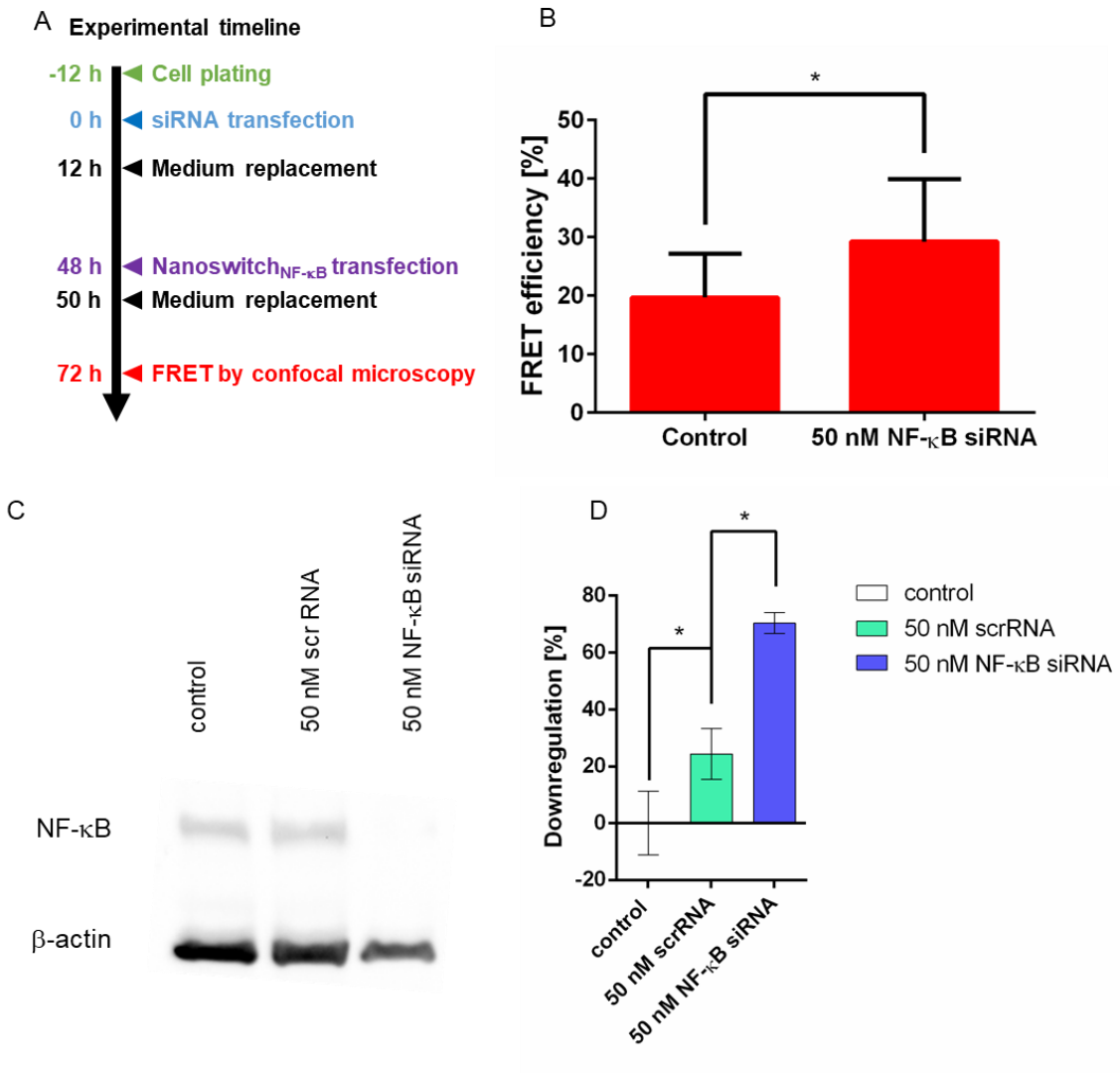

Figure S12. (A) Schematic illustration of the experimental timeline: cells were transfected with siRNA targeting NF-κB to downregulate protein expression. After 48 h, cells were subsequently transfected with the Nanoswitch$_{\text{NF-κB}}$ and the changes in protein concentration were measured by confocal microscopy. (C) Intracellular FRET measurements in PC3 cells transfected with 50 nM siRNA targeting NF-κB, followed by 25 nM Nanoswitch$_{\text{NF-κB}}$ transfection, n = 100. (C) Representative Western Blot of siRNA-mediated NF-κB downregulation in PC3 cells compared with cells transfected with scrambled siRNA (scrRNA, negative control). (D) Histogram reporting siRNA-mediated NF-κB downregulation in PC3 cells after transfection for 48 h with lipofectamine–siRNA formulation. Error bars represent standard deviations, n = 2. Statistically significant difference was determined by a student t-test and is reported as *$p < 0.05$.

Section S4. Cell viability assay.

Cells viability was measured using the MTT assay. PC3 cells were seeded at a seeding density 1×10^4 cells/well on a 96-well plate (Costar 3569, Corning, MA, USA) in 100 µL DMEM medium supplemented with 10% fetal bovine serum (FBS) and grown overnight. Then, the media was discarded, and cells were transfected with lipofectamine RNAiMAX only, complexes of lipofectamine RNAiMAX/control FRET sequence, or complexes of lipofectamine RNAiMAX/Nanoswitch$_{\text{NF-κB}}$ in OPTI-MEM media. After 2 h, the transfection medium was replaced with DMEM medium supplemented with 10% FBS. The MTT reagent was added at either the 2 h or the 24 h mark for incubation for 4 h. The resulting formazan crystals were dissolved in dimethyl sulfoxide and the absorbance of solution was measured at 554 nm with reference measurement at 670 nm on an Infinite M200 microplate reader (Tecan, Switzerland).

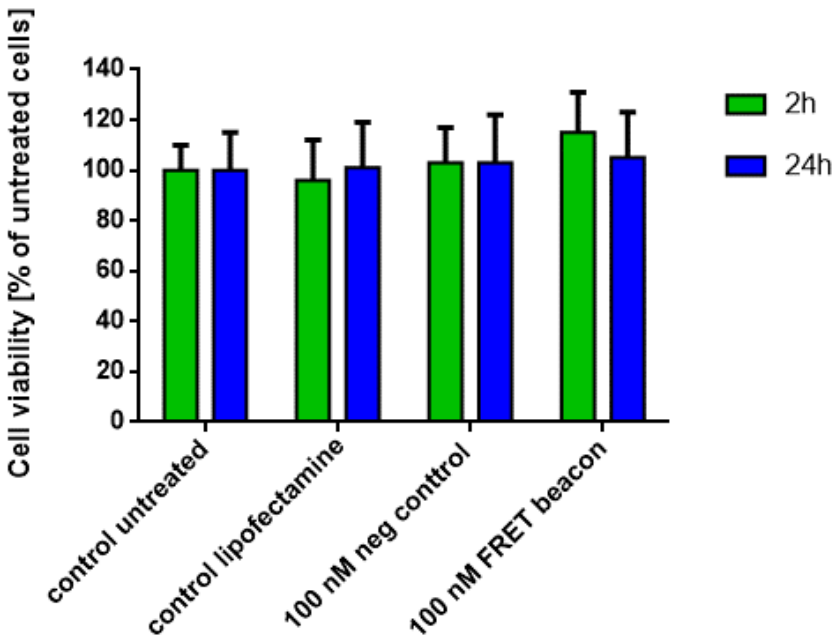

Figure S13. The histogram compares cell viability between non-transfected cells, cells transfected with Lipofectamine RNAiMAX only, 100 nM control FRET sequence, or 100 nM Nanoswitch$_{\text{NF-κB}}$. MTT test was performed after transfection for 2 and 24 h in triplicates. Error bars represent standard deviations, $n = 3$.

Section S5. Enzyme-linked immunosorbent assay (ELISA).

For the ELISA, human prostate cancer PC3 cells were plated on a 24-well plate (Costar 3524, Corning, MA, USA) at a seeding density of 4×10^4 cells per well in 500 µL of DMEM medium supplemented with 10% FBS and incubated at 37 °C in 5% CO_2 overnight. Then, transfection with the Nanoswitch$_{\text{NF-κB}}$ was performed in OPTI-MEM reduced serum medium, using lipofectamine RNAiMAX as a carrier as per supplier protocol, with a final DNA concentration of 50 nM. After incubation for 2 h with Nanoswitch$_{\text{NF-κB}}$/lipofectamine RNAiMAX complexes, the transfection medium was discarded, and cells were washed with sterile D-PBS and incubated in fresh culture medium for another 0, 5, 8 and 22 h (corresponding to final time points of 2, 7, 10 and 24 h). Then, cells were processed using Abcam NF-κB in vitro SimpleStep ELISA™ kit as per manufacturer protocol. The final measurements were performed on a microplate reader.

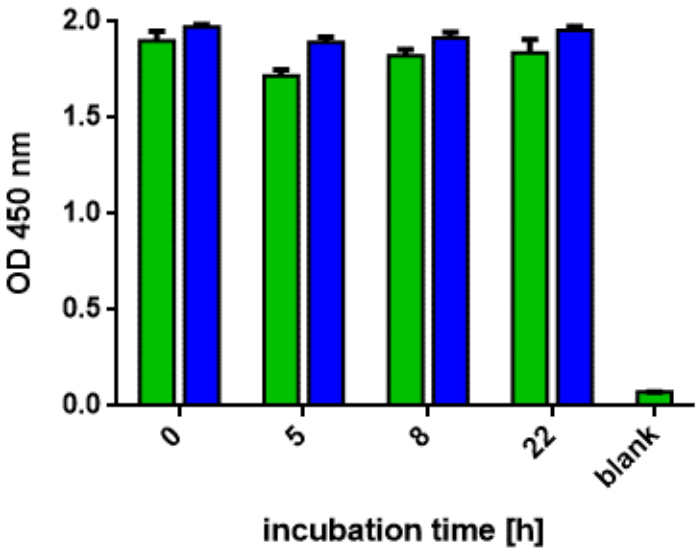

Figure S14. PC3 cell extract analysis for total p65 NF-κB. Green bars indicate the absorbance (measured at λ = 450 nm) of cells following transfection with Nanoswitch$_{\text{NF-κB}}$ at different time points (2, 7, 10, and 24 h). Blue bars represent the absorbance (measured at λ = 450 nm) of non-transfected cells, incubated for the same amount of time. Data from triplicate measurements are plotted and compared to 1× cell extraction buffer (blank). Error bars denote standard deviations. Adapted with permission from Bertucci *et al.*[2] Copyright 2018 Royal Society of Chemistry.

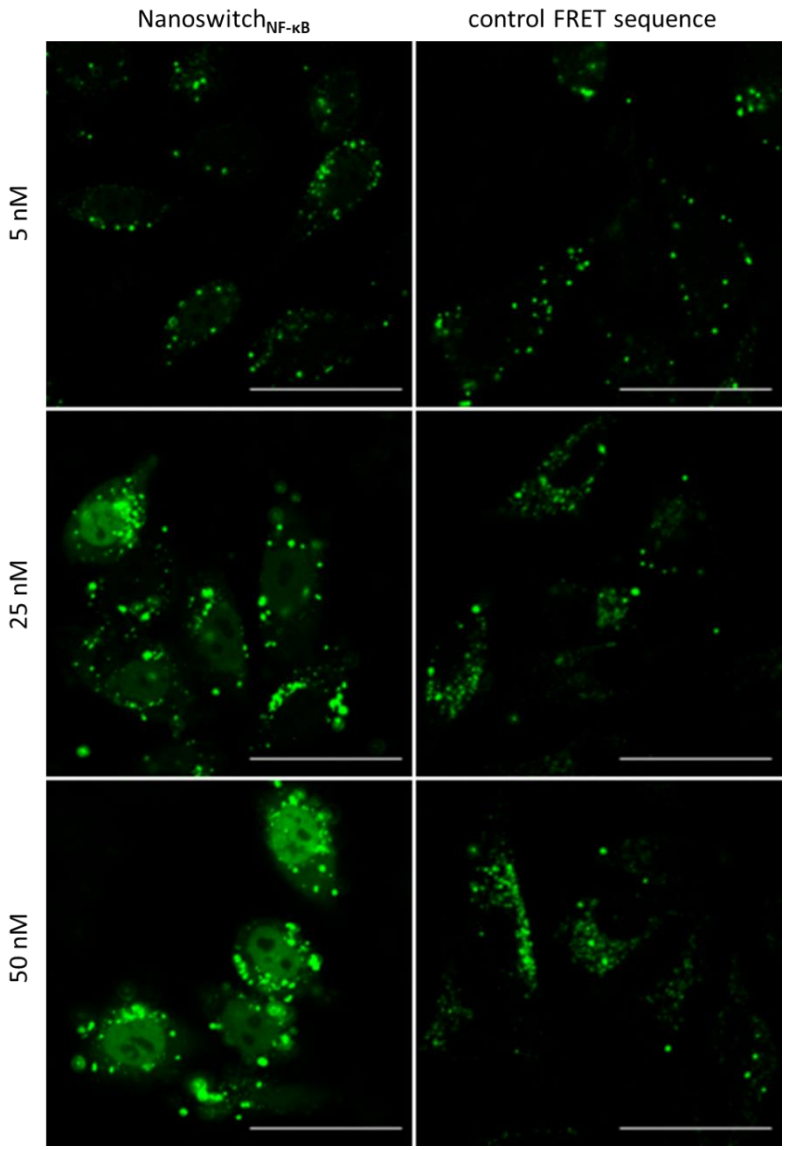

Figure S15. Representative confocal microscopy images of PC3 cells transfected with 5, 25, or 50 nM Nanoswitch$_{NF-κB}$ or control FRET sequence imaged live after 4 h. The dim fluorescence signal of the control FRET sequence was acquired using a higher laser intensity. Scale bars = 50 μm.

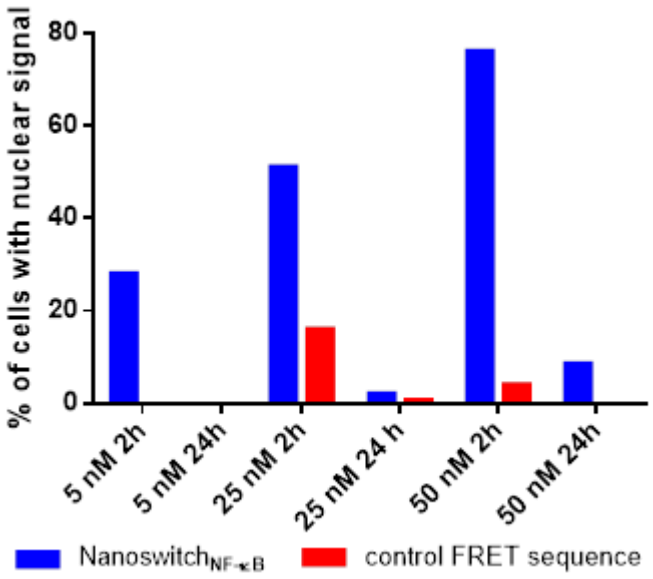

Figure S16. Percentage of live cells presenting a nuclear fluorescent signal. Cells were transfected with Nanoswitch$_{NF-\kappa B}$ and control FRET sequence at a concentration of 5, 25, or 50 nM for 2 h, followed by additional 2 h and 22 h incubation in fresh culture media, then live-imaged. For each condition, at least 100 cells were analyzed**.**

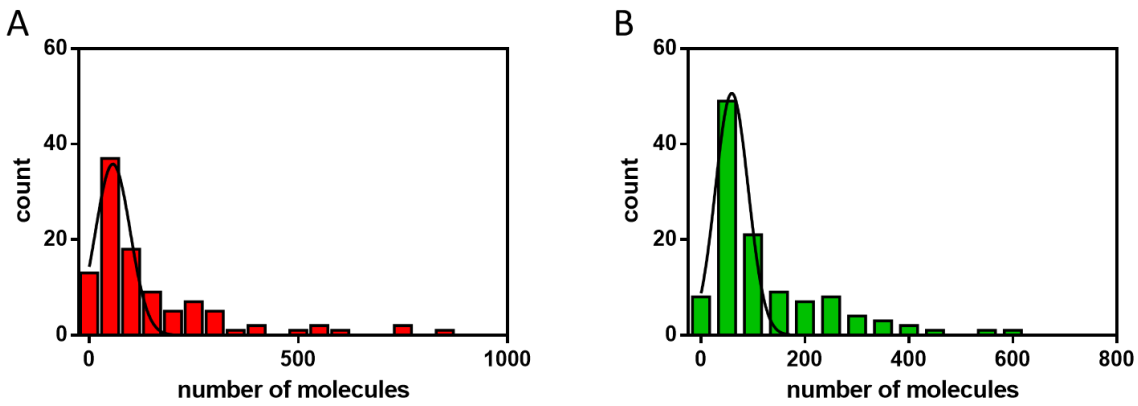

Figure S17. Number of localizations events identified within imaged (A) Nanoswitch$_{\text{NF-κB}}$ and (B) NF-κB p50 molecules; n = 100.

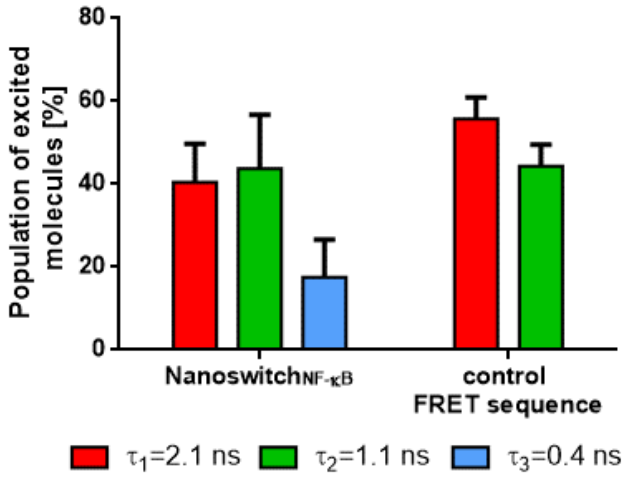

Figure S18. Distribution of identified populations of fluorescence lifetimes within PC3 cells transfected with 50 nM Nanoswitch$_{\text{NF-κB}}$ or control FRET sequence for 2 h. Error bars indicate standard deviations; n = 20.

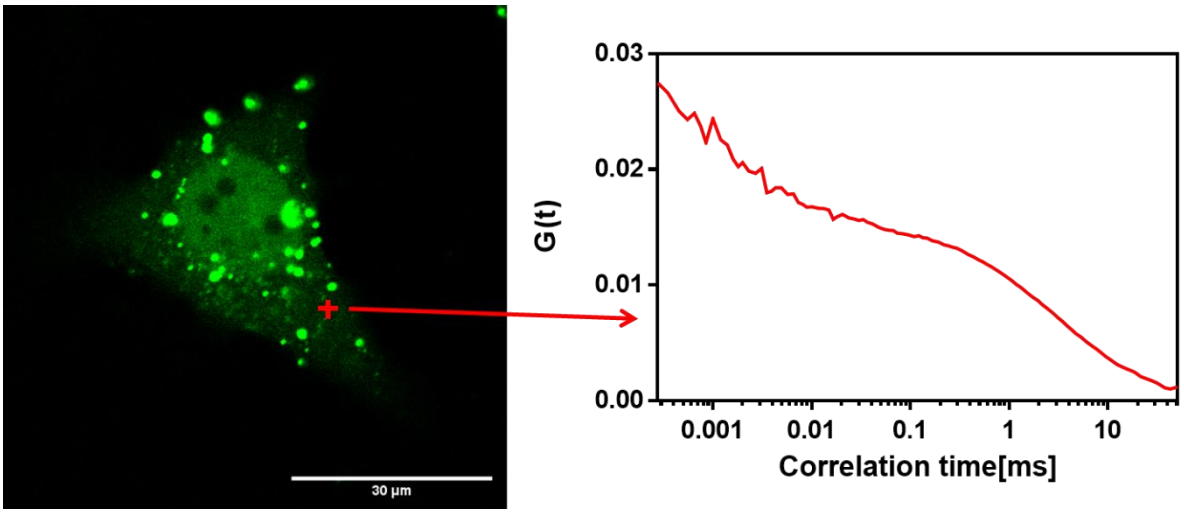

Figure S19. Experimental set up for fluorescence correlation spectroscopy (FCS) measurements performed at 10 various points in every cell. All of the measurement data were analyzed by fitting with the anomalous diffusion model including the triplet dynamic and two components in 3D, and the data obtained are presented in Table 1.

References

(1) Zadeh, J. N.; Steenberg, C. D.; Bois, J. S.; Wolfe, B. R.; Pierce, M. B.; Khan, A. R.; Dirks, R. M.; Pierce, N. A. NUPACK: Analysis and Design of Nucleic Acid Systems. *Journal of Computational Chemistry* **2011,** *32* (1), 170.

(2) Bertucci, A.; Guo, J. L.; Oppmann, N.; Glab, A.; Ricci, F.; Caruso, F.; Cavalieri, F. Probing transcription factor binding activity and downstream gene silencing in living cells with a DNA nanoswitch. *Nanoscale* **2018,** *10* (4), 2034.